# PURIFICATION AND STRUCTURAL CHARACTERIZATION OF THE EPITHELIAL SODIUM CHANNEL

THESIS

Presented to the Graduate Council
of Texas State University – San Marcos
in Partial Fulfillment
of the Requirements

for the DEGREE

Masters of SCIENCE

by

Sean Larson Schmidt, B.S.

San Marcos, Texas
May 2006

ACKNOWLEDGEMENTS

Many people helped me along the way in completing the work needed for this thesis. I can not thank Dr. Rachell Booth enough for all of her assistance, guidance, and knowledge in helping me complete my work. I came into this program knowing very little about biochemistry and lab techniques. Dr. Rachell Booth took the time to explain and assist me in every aspect of lab work. I would also like to thank my committee members, Dr. Lysle Kevin Lewis and Dr. Walter Rudzinski for their time and efforts. Fellow graduate students also offered a helping hand when needed, including Tzyy-Jing Chuang (George), Amy Perez, Hiranthi Thambugala, and Jared Cassiano. The undergraduates in the lab deserve acknowledgement as well. Carter Mitchell, Gabrielle Moreno, and Roberto Perales helped out whenever needed around the lab. Dr. Jim Stockand's research lab at the San Antonio Health Science Center was helpful in providing materials in times of dire necessity. My appreciation also goes to the College of Science and the Department of Chemistry and Biochemistry for their financial support.

My parents were a tremendous help. Their financial support for tuition and living expenses during my commute to and from Houston would not have been possible without them. They saw potential in me from little on and have always pushed for me to be all that I can be, and spared no expense for me to do so. My loving wife is like no other. Throughout all of my education that I have known her, she has helped me to learn better study habits, manage my time more efficiently, and always offered great words of advice.

Finally, I would also like to thank God for giving me the ability to accomplish as much as I have. Thank you to all who have helped me succeed to where I am today.

This manuscript was submitted on January 17, 2006.

TABLE OF CONTENTS

## LIST OF TABLES

**Table**

## LIST OF ILLUSTRATIONS

**Figure**

## LIST OF ABBREVIATIONS

| | |
|---|---|
| α | Alpha subunit |
| AMP | Ampicillin |
| Arg | Arginine |
| β | Beta subunit |
| BSA | Bovine Serum Albumin |
| Ca | Calcium |
| CAP1 | Channel Activated Protein |
| CM | Carboxymethyl exchange groups |
| COS-1 | Green Monkey Kidney cells |
| DE52 | Diethylaminoethyl Cellulose |
| $dH_20$ | Deionized water |
| DNA | Deoxyribonucleic acid |
| DTBP | dimethyl-3-3.-dithiobispropionimidate |
| DTT | Dithiothreitol |
| *E coli* | *Escherichia coli* |
| ENaC | Epithelial Sodium Channel |
| FBS | Fetal bovine serum |
| FT | Flow Through |
| H | Hydrogen |
| g | gram |
| K | Potassium |
| kDa | Kilo Dalton |
| $K_i$ | half-inhibition constant |
| γ | Gamma subunit |
| GLB | Gentle Lysis Buffer |
| Gln | Glutamine |
| IP | Immunoprecipitation |
| L | Liter |
| LB | Luria-Bertani |
| Li | Lithium |
| Lys | Lysine |
| M | Molarity |
| mg | Milligram |
| mL | Milliliter |
| mM | Millimolar |
| MR | Mineralocorticoid receptor |
| Mg | Magnesium |

| | |
|---|---|
| Na | Sodium |
| NaCl | Sodium Chloride |
| $NaHCO_3$ | Sodium bicarbonate |
| $NH_3$ | Amino |
| Ni | Nickel |
| PAGE | Polyacrylamide gel electrophoresis |
| pCMV-Myc | Mammalian expression vector-Myc tag |
| PBS- | Phosphate Buffered Saline (-Ca and -Mg) |
| PBS++ | Phosphate Buffered Saline (-Ca and -Mg) |
| PHAI | Pseudohypoaldosteronism type 1 |
| PMSF | Phenylmethyl Sulfonyl Fluoride |
| rpm | Revolutions per minute |
| SDS | Sodium dodecyl sulfate |
| TBST | Tris-buffered saline plus tween |
| TBS | Tris-buffered saline |
| Tris | Tris(hydroxymethyl) amino methane |
| µg | Microgram |
| µL | Microliter |
| W | Wash |
| WCL | Whole cell lysate |

ABSTRACT

PURIFICATION AND STRUCTURAL CHARACTERIZATION OF THE EPITHELIAL SODIUM CHANNEL

By

Sean Larson Schmidt, B.S.

Texas State University-San Marcos

May 2006

SUPERVISING PROFESSOR: RACHELL E. BOOTH

The formation and regulation of transport channels within mammalian cells are directly related to their proper function. The epithelial sodium channel (ENaC) is responsible for regulating sodium reabsorbtion within the distal tubule of the nephron of the kidney. Gain-in-function mutations in ENaC cause prolongation of the time the channel remains in the plasma membrane resulting in hypertension. Understanding function of this channel and its abnormal behavior that causes disease requires knowledge of the channel complex structure. Previous studies have demonstrated that there are 3 distinct, but homologous subunits: $\alpha$, $\beta$, and $\gamma$. However, there is contradicting evidence on the subunit composition of this channel with two differing proposals of a 4-subunit

and 9-subunit channel complex. We examined the subunit composition of ENaC using several traditional biochemistry techniques including crosslinking, affinity chromatography, cation and anion exchange chromatography, and polyacrylamide and agarose electrophoresis. For crosslinking, we covalently linked amino functional groups of lysine residues that are in close proximity. Native and denaturing polyacrylamide gel electrophoresis gels were used to determine if the subunits were crosslinked, and agarose gels to visualize the crosslinked complexes. The results were not consistent with predictions of a 4-subunit model. By examining the structure of ENaC, we will be aiding future research in the possible manipulation of the channel to treat or prevent diseases.

# CHAPTER 1

## INTRODUCTION AND LITERATURE REVIEW

Protein-protein interactions play a central role in many biological processes. The activities of intrinsic membrane proteins, for instance, are often regulated by the formation of protein-protein interactions with regulatory and accessory proteins (1). The Epithelial Sodium Channel (ENaC), a pore forming membrane protein found in the kidney, mediates sodium reabsorption. ENaC is also located in the apical membrane of other epithelial tissues throughout the body, including the nephron, colon, lungs, sweat glands airway, and other epithelia. In the lung, ENaC activity is necessary for fluid handling, in particular at birth, when the transition from a liquid-filled to air-filled lung occurs (2).

The kidneys regulate blood composition by three main processes: filtration, reabsorption, and secretion. In the nephron, the basic unit of the kidney, (a long thin tube that is closed at one end, has two twisted regions interspaced with a long hairpin loop, ends in a long straight portion, and is surrounded by capillaries) approximately 20 percent of the blood gets filtered under pressure through the walls of glomerular capillaries and Bowman's capsule (closed end at the beginning of the nephron). The filtrate is composed of water, ions (i.e. sodium, potassium, and chloride), glucose, and small proteins. Once inside the lumen of the nephron, small molecules, such as ions, glucose and amino acids, get reabsorbed from the filtrate as needed. There are three factors that contribute to the

effectiveness of the reabsorption, including concentration of ions, quantity of transporters, and rate of filtrate. As the concentration of particulates increases, a concentration gradient across the membrane is established. This will aid in the transport of these particulates, leading to additional reabsorption. The quantity of transporters directly effect reabsorption as well. An increased number of transporters will increase reabsorption, and vise versa. The final factor that affects the reabsorption process is the rate of flow of the filtrate. Flow rate affects the time available for the transporters to reabsorb molecules before they are carried into the bladder.

The proximal tubule of the nephron reabsorbs 65 percent of filtered $Na^+$, the Loop of Henle (long hairpin loop after the proximal tubule extending from the cortex down into the medulla and back) reabsorbs 25 percent of filtered $Na^+$, distal tubule (second twisted portion of the nephron after the loop of Henle) reabsorbs 8 percent of filtered $Na^+$, and finally the collecting duct (long straight portion after the distal tubule which is the open end of the nephron extending from the cortex down through the medulla) reabsorbs up to 2 percent of the remaining sodium.

The kidney maintains the proper extracellular fluid volume in the body, in part, through modulation of $Na^+$ reabsorption in the nephron (18). ENaC is located in the apical membrane (Figure 1) of the epithelial cells composing the distal tubule and collecting duct of the nephron and is the rate-limiting step in $Na^+$ reabsorption.

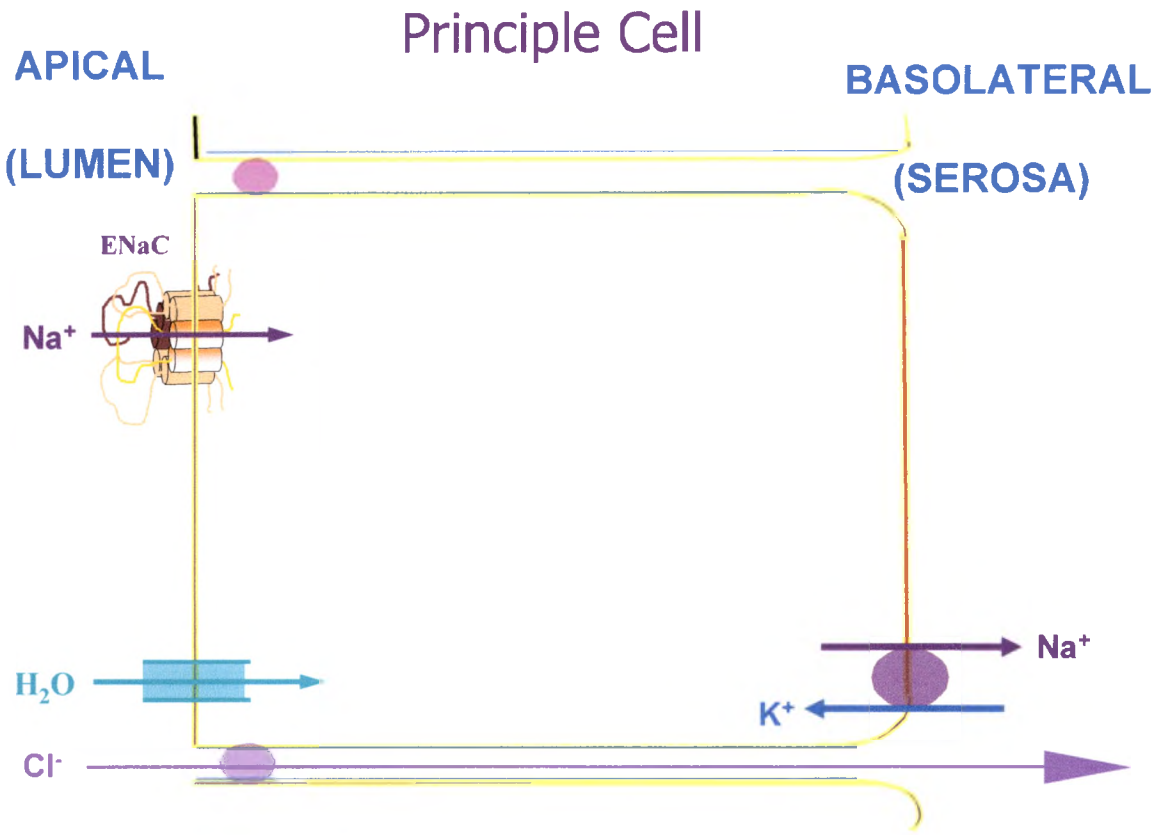


*Figure* 1: **ENaC Location in an Epithelial Cell**

Since sodium reabsorption in the distal tubule and collecting duct is regulated via ENaC, mutations in a PPXY motif on the carboxyl -terminal of the gamma subunit increase the time the channel resides in the plasma membrane, ultimately increasing the effective channel number that causes an increase in sodium retention and hypertension (high blood pressure) (14). The role of $Na^+$ channels in blood pressure regulation has been in studies that have identified genetic mutations in ENaC as the basis for the pathogenesis of Liddle's disease, a disorder characterized by volume expansion and hypertension, as well as type I pseudohypoaldosteronism, a disorder characterized by volume depletion and hypotension (8).

Abnormalities in the function of this channel, linked to genetic alterations in channel protein sequence, have been shown to be important in several human diseases, including hypertension seen in patients with Liddle's syndrome, and salt-washing seen with some variants of pseudohypoaldosteronism. Hypertension or elevated arterial blood pressure is a substantial public health problem, affecting 25 percent of the adult population in industrialized societies, which affects 50 million Americans and contributes to over 200,000 deaths annually from stroke, myocardial infarction, and end-stage renal disease. While ENaC's role in hypertension is unclear, it is not the single determinant of hypertension in the vast majority of subjects (10).

Liddle's Syndrome, an inherited form of hypertension, is characterized by autosomal dominant transmission of early onset hypertension associated with hypokalemic alkalosis, suppressed plasma rennin activity, and low plasma aldosterone levels. This disease is caused by mutations in either β- or γ-ENaC in which the cytoplasmic carboxyl-termini is altered. This results in an increase in ENaC activity, mainly attributed to an increase in the number of channels at the cell surface. The increased number of channels is due to a reduction in retrieval of ENaC from the cell surface. These mutations introduce frameshifts or premature stop codons that delete the intracellular carboxyl-regulatory terminal domains of the β- or γ-subunits, or they substitute residues in a motif present in the carboxyl termini of both subunits. Expression of ENaC channels with truncated β- or γ-subunits in *Xenopus* oocytes induces amiloride-sensitive whole-cell currents 3-5 fold larger than the wild type channels (4, 5, 13, 17). An increase in the open probability and the number of channels expressed at the cell

surface are the two possible mechanisms proposed to explain the increase in sodium reabsorbtion due to Liddle's syndrome.

Pseudohypoaldosteronism type 1 (PHA-1) features severe neonatal salt washing with hypotension despite elevated aldosterone levels. Although aldosterone has been shown to increase the activity of ENaC, activity of ENaC is not regained even with elevated amounts of aldosterone. The partial loss of the mineralocorticoid receptor (MR), the receptor for aldosterone, impairs maximal salt reabsorbtion. Loss-of-function in any of the three different ENaC subunits causes the autosomal recessive form of PHAI. Just like the dominant PHAI, the recessive form features life-threatening salt wasting and hypotension in the neonatal period with hyperkalemia and metabolic acidosis (11).

The lack of adequate blood pressure control among a large number of hypertensive patients remains a major public health concern. The importance of maintaining blood pressure control is of great concern to patients who are at substantial risk for organ damage, including patients with additional conditions such as renal disease and diabetes. Thus, improved blood pressure control through advances in treatment strategies and pharmacologic agents remains a significant unmet need. By fully understanding the structure/function relationship of ENaC, we can attempt to overcome these health concerns through production of proper medications.

ENaC is highly selective for $Na^+$ ions over $K^+$ ions ($P_{Na+}/P_{K+} = 100$). With the exception of $Li^+$ ($Li^+/Na^+$: 1.5/1.0), which is more permeable than $Na^+$, no other monovalent cations permeate the channel (14). ENaC belongs to a large family of cation channels known as the ENaC/degenerin (DEG) which also include several mammalian acid-activated channels expressed in the nervous system, the degenerins from

*Caenorhabditis elegans* involved in the transduction of machanosensitive stimuli, and the neuropeptide-activated channel from the ganglion of *Helix aspersa* (1, 16).

A family of genes identified in *Caenorhabditis elegans* based on mutations that result in mechanosensation defects (MEC's) and degeneration of selected neuronal cells (DEG's) are structurally related to the genes of ENaCs. Several of these genes, including mec4, mec6, and mec10, are thought to form ion channels analogous to the three ENaC subunits (8). Members of the ENaC/degenerin family are homo- or hetero- oligomeric proteins whose subunits share a common topology of two membrane spanning domains (M1 and M2) and intracellular amino and carboxyl termini (Figure 2) (16).

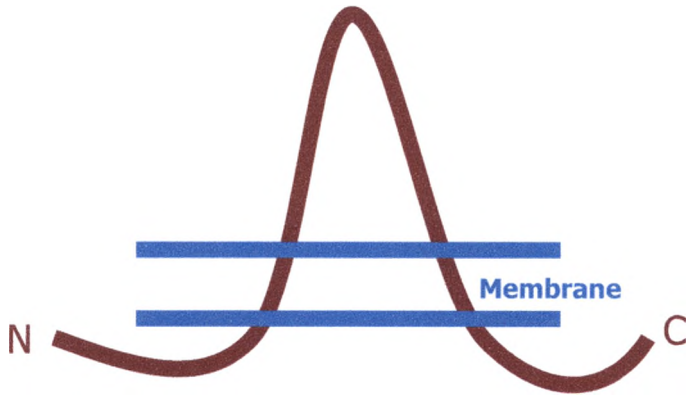


*Figure* 2: **Domains and Termini of a Single Subunit** Each subunit contains two transmembrane domains, a large extracellular loop, and cytoplasmic N- and C-termini.

ENaC channels are composed of three homologous but distinct subunits designated as α-ENaC, β-ENaC, and γ-ENaC that share 34-37% identity at the amino acid level (Figure 3) (4).

The ENaC subunits, like most membrane proteins, are glycoproteins of 75 to 90 kDa (14). Although all three subunits of ENaC are found in normal channels, sodium

currents have been produced *in vitro* using the α-subunit alone. Co-expression of α-ENaC with both β- and γ-subunits resulted in currents 100 fold higher than α-ENaC alone (9). Various combinations of subunits including αβ, αγ, or α alone form channels with distinct electrophysiological properties (1). These same studies have shown that neither β nor γ-ENaC alone have the ability to form functional channels (10). The pore of ENaC has several important characteristics. Pore properties include: selectivity, gating, conductance, and the binding of channel blockers (2). In contrast, the hydrophobic domains of ENaC subunits are predicted to have an α helical structure, similar to the sixth transmembrane domains of voltage-gated $K^+$, $Na^+$, and $Ca^{2+}$ channels and to the second transmembrane domains of inward rectifier $K^+$ channels. Recent work suggests that M2, (the membrane spanning region near the carboxyl terminal) domains of ENaC also contribute to the formation of the pore. Mutations of the negative-charged amino acids within the M2 domains of human α-ENaC nearly eliminated channel activity, while leaving protein expression levels at the plasma membrane unaffected (16).

The subunit composition of ENaC is unknown. One proposed stoichiometry of ENaC's subunits is 2α: 1β: 1γ with all of the subunits contributing to the pore (Figure 3) (5, 12). Kosari's lab suggests a tetrameric channel of 2 alpha to every one beta/gamma based on a biophysical assay which utilized mutant subunits displaying significant differences in sensitivity to channel blockers when compared to the wild type channel (12). In addition, Firsov's lab also suggests a 4-subunit stoichiometry channel based on their expression of concatameric cDNA constructs made of differing combinations of ENaC subunits (5).

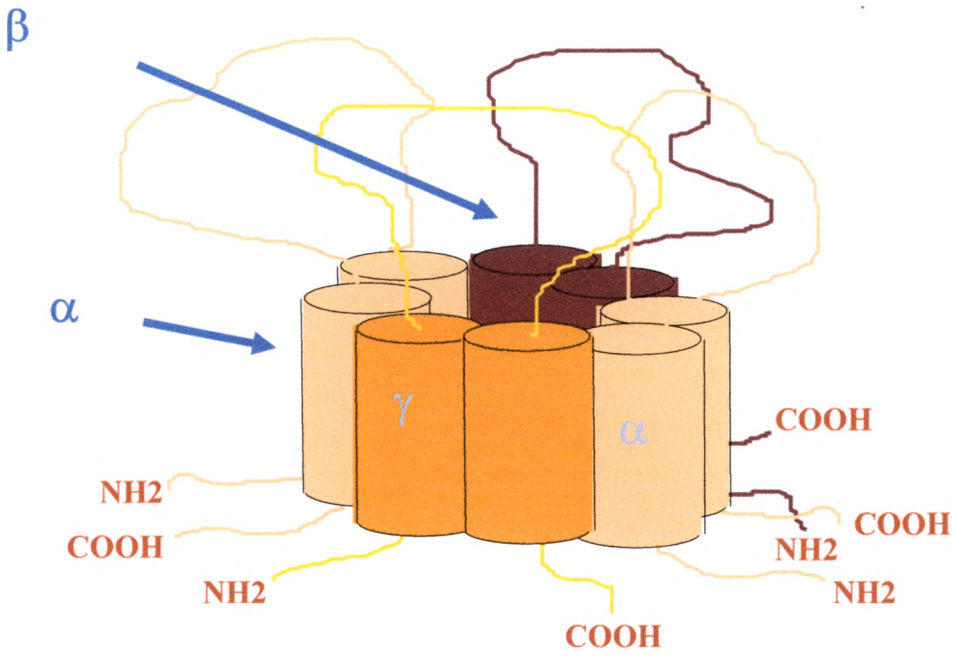


*Figure* 3: **4-Subunit Model** Each subunit contains two transmembrane domains, a large extracellular loop, and cytoplasmic N- and C-termini.

An alternate stoichiometry of 3α: 3β: 3γ has also been proposed (Figure 4) (3, 22). Eskandari's lab suggests an eight or nine-subunit channel based on their freeze-fracture electron microscopy and electrophysiological methods used to evaluate the number of subunits in the ENaC complex expressed in Xenopus laevis oocytes (3). Also supporting this model is Snyder's lab who expressed the three wild type subunits with subunits containing mutations that alter channel inhibition by methanethiosulfonates (22).

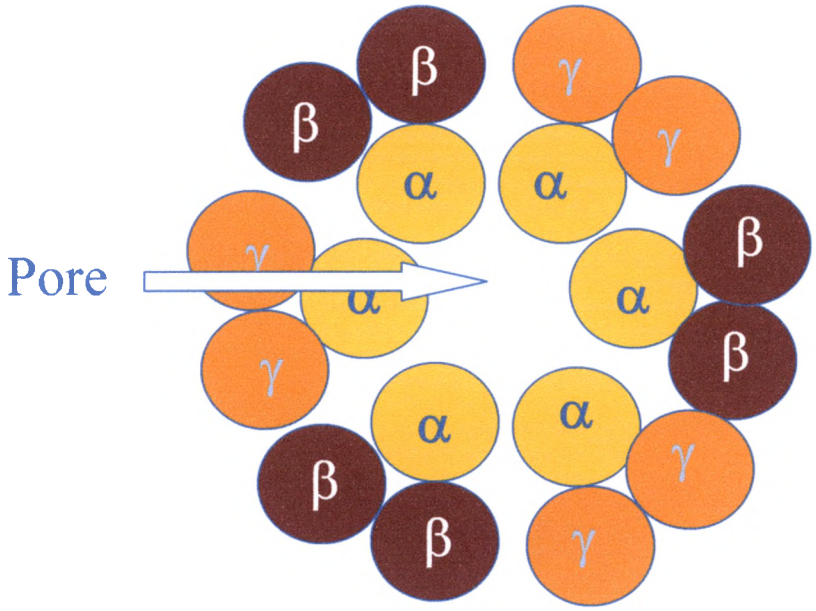


*Figure* 4: **9-Subunit Model** Each subunit contains two transmembrane domains, a large extracellular loop, and cytoplasmic amino and carboxyl termini.

Selected mutations within the pore region alter ion selectivity, or single channel conductance, as well as amiloride sensitivity. For example, a critical 3-residue (G/S) XS (where X is Ser, Gly, or Cys) tract within each subunit appears to primarily govern ENaC selectivity (9). Each ENaC subunit is comprised of two transmembrane domains, a large ectomain flanking them containing numerous amino-linked glycosylation sites, and short intracellular amino and carboxyl termini (4, 17). The amino-termini of α- and γ-ENaC contain conserved Lys residues that serve as ubiquitin acceptor sites (17). All three ENaC subunits are glycosylated and indeed mutation of all N-linked glycosylation sites in α-ENaC does not seem to affect channel function (2).

The channel is regulated by hormones such as aldosterone, vasopressin, insulin, and antidiuretic hormone that increase its activity by diverse mechanisms including increase in channel synthesis, incorporation of channels from an intracellular pool to the

plasma membrane, and post-translational modification of the channel (17). ENaC is stimulated when the T628 on the carboxyl-terminal of the gamma subunit is phosphorylated by MAPK. Channel activated protease (CAP1), Nedd4 (ubiquitin ligase), and CFTRT are proteins that have been shown to directly or indirectly interact with ENaC and modulate its activity (7, 14). When the three WW domains on Nedd4 interact with the conserved PPXY motif on the carboxyl-terminal of the gamma or beta subunit, ENaC is retrieved from the membrane and targeted for degradation. ENaC is also retrieved from the membrane and targeted for degradation when the CAP-1 interacts with the endocytic YXXL tag on the carboxyl-terminal of the gamma and beta subunit. Previous research suggests that the carboxyl terminus of the channel subunits operate in processes that normally down-regulate its activity.

Structural studies of the ENaC/degenerin family of ion channels have been hampered so far by the uncertainty in removing them from the membrane environment with out disrupting structure and obtaining sufficient quantities of these proteins. In native tissues, ENaC has low expression levels, permitting electrophysiological and limited immunufluoresence analysis to be performed but precluding biochemical studies (5).

Structure-function relationships are important in understanding the central role in many biological processes. Examining ENaC's structure through the use of traditional biochemistry techniques including protein purification and chemical crosslinking will help us to understand these structure-function relationships. In future studies, isolated protein from this work will be analyzed via peptide mass mapping in order to identify additional motifs in ENaC which can be manipulated and functionally characterized.

These future findings will give insight to ENaC's role in homeostasis and blood pressure regulation.

# CHAPTER II

# MATERIALS AND METHODS

## DNA Materials And Methods

### Transformation

#### Top 10 cells (Invitrogen)

Frozen cells were thawed on ice for 10 minutes. A mixture of 100 µL cold KCM buffer (100 mM KCl, 30 mM $CaCl_2$, and 50 mM $MgCl_2$), 1 µg plasmid DNA, and 100 µL thawed *E. Coli* competent cells were mixed and incubated on ice for 10-20 minutes. The mixture was then warmed to 25-30°C for 10 minutes. LB broth (10.0 g/L pancreatic digest of casein, 5.0 g/L yeast extract, and 5.0 g/L NaCl) was added and the transformation reaction was agitated at 225 rpm for 40-60 minutes at 37°C. The cells were then spread on LB-ampicillin agar plates (10.0 g/L peptone from casein, 5.0 g/L yeast extract, 10.0 g/L NaCl, 12.0 g/L agar-agar and 100 µg /ml ampicillian).

### Overnight Cultures

One colony was placed into a LB broth with 100 µg/ml of ampicillin (100 mg/ml) and incubated (Orbit Environ Shaker – LabLine) overnight at 225 rpm at 37°C.

**Plasmid Isolation**

All plasmids were isolated with Qiagen's HiSpeed™ Plasmid Midi kit per manufactures instructions. A single colony from a streaked plate was selected and incubated in 150 mL LB medium and antibiotic overnight at 37°C to form a starter culture. The cells were then harvested by centrifugation (Beckman J2-21) at 6000 x g for 25 minutes at 4°C. The pellet was resuspended in 10 mL buffer P1. Buffer P2 (10 mL) was added, gently mixed, and incubated at room temperature for 5 minutes. Chilled buffer P3 (10 mL) was added to the lysate and mixed immediately. The lysate was then poured into the barrel of a QIAfilter Cartridge and incubated at room temperature for 10 minutes. The lysate was then forced through the cartridge into a HiSpeed Tip via an included plunger. The cleared lysate was allowed to enter the resin by gravity flow. The tip was washed with 60 ml Buffer QC. The DNA was then eluted with 15 mL Buffer QF. The DNA was precipitated by adding 10.5 mL room temperature isopropanol to the eluted DNA, mixed, and let incubate at room temperature for 5 minutes. The bound DNA was washed by forcing 70% ethanol through the included precipitator and eluted with 15 mL Buffer QF.

**DNA Quantification**

DNA was quantitated using a Hoefer DyNA Quant 200 flourometer. Buffer A (45 mL water, 1 X TNE and 10 μL Hoechst 33258) was added to a clean glass cuvette and used to zero the machine. Calf Thymus DNA standard (100 ng/μL) was used for calibration. The samples were read with an excitation spectrum at 356 nm and an emission spectrum at 492 nm.

**Transfection**

After COS-1 cells were passed and confluency was less than 40%, the cells were transfected. For each plate, 1.5 μg DNA was diluted into 300 μL Dulbecco's Modification of Eagles Medium-0 (incomplete media without L-Glutamine, Fetal Bovine Serum, and Penicillin-Streptomycin). Twenty-five micro liters of Qiagen Polyfect® Transfection Reagent was added and vortexed for 10 seconds. The transfection reaction was incubated at room temperature for ~10 minutes. Old media was removed from cells and the cells were rinsed with 10 mL PBS- (Phosphate Buffered Saline without Mg and Ca). Seven milliliters of complete media [Dulbecco's Modification of Eagles Medium 1 X with (Mediatech Cellgro), L-Glutamine powder (Mediatech Cellgro), Fetal Bovine Serum characterized 40 nm filtered (HyClone®), and Penicillin-Streptomycin 10,000 ug/mL (Mediatech Cellgro™)] was added to DNA mixture and mixed by pipetting. This DNA mixture was then added to the cells and incubated in a 5% $CO_2$ incubator (VWR Scientific Products 1535) at 37°C for 48 hours.

## Protein Materials And Methods

**Purification**

**Harvesting Cells**

Media with transfection reaction was removed 48 hours after transfection and cells were washed twice with PBS-. A stock 1/27,708 dilution of phenylmethyl sulfonyl fluoride (PMSF) solution was made in 100 % ethanol. A 1/200 dilution of this stock was made into GLB. Two-hundred-fifty micro liters of this PMSF/GLB stock were added to

each plate to lyse the cells. Cells were then scraped off the bottom of the dish and incubated at 4°C. Cell debris was spun down at ~2,040 x g for 5 minutes and pellet discarded.

**Dialysis**

Total protein from harvesting was dialysised with Spectrapor® Membrane Tubing 3,500 MW cut-off tubing. The buffer consisted of 50 mM NaCl, 0.3 M monobasic $Na_2HPO_4$, pH 8.0. The sample was placed into buffer and stirred at 4°C for 1 hour. The buffer was replaced and stirred at 4°C for 5 hours, then replaced again for overnight stirring at 4°C.

**Affinity Chromatography – Full Column**

ENaC was partially purified using a His-Select™ Nickel affinity gel column (Sigma). (ENaC α-subunit has engineered His6 tagged for affinity to Ni). Ni-NTA agarose resin (Invitrogen), ~1.5 mL, was spun for 30 seconds at 14,000 rpm, removed top ethanol layer, and resuspended with equilibration buffer: 50 mM $NaH_2PO_4$ pH 8.0 with 0.3 M NaCl. The column was equilibrated with 3 column volumes of equilibration volumes. One milliliter of unpurified whole cell lysate kept from extraction. Whole cell lysate containing ENaC was passed through the column. The column was washed with 6 column volumes 50 mM $NaH_2PO_4$, 0.3 M NaCl, pH 8.0, and 10 mM Imidizole. ENaC was eluted with 50 mM $NaH_2PO_4$, pH 8.0, with 0.3 M NaCl and 250 mM Imidizole. Fractions were collected in 0.5-1 mL increments and stored at 4°C. The column was regenerated with 6 M Guanadine HCl buffer, pH 7.5.

**Affinity Chromatography – Spin Columns**

ENaC was also partially purified using a His-Select™ Spin Column (Sigma). The column was equilibrated by spinning 600 uL equilibration buffer (0.1 M sodium phosphate and 8 M urea, pH 8.0) through at 2,040 x g for 2 minutes. Whole cell lysate (600 uL) containing ENaC was spun through the column at 2,040 x g for 2 minutes. Unbound protein wash washed from the column by spinning 600 uL wash buffer (same as equilibration buffer) at 2,040 x g for 2 minutes two different times. Protein was eluted with 500 uL elution buffer (0.1 M sodium phosphate with 8 M urea and 250 mM imidazole, pH 8.0) by spinning at 2,040 x g for 2 minutes. The spin columns were discarded after each use.

**Cation Exchange Chromatography**

CM cation exchange cellulose resin, 250 µL, (BIO-RAD Cellex®-CM) was washed 10 times with 0.2 M Tris-HCl, pH 8.0. ENaC fractions from the nickel column (alpha subunit only) were then added to the resin and agitated for 30 minutes at room temperature. The supernatant was removed and saved for analysis. The resin was washed 6 times with 0.2 M Tris-HCL, pH 8.0. The protein was then eluted with a 1 M NaCl in 0.2 M Tris-HCl. The tube was agitated for 30 minutes at room temperature. All samples were stored at 4°C.

**Anion Exchange Chromatography**

DE52 pre-swollen anion exchange cellulose resin, 250 µL, (Whatman® International Ltd) was washed 10 times with 0.2 M Tris-HCl, pH 8.0. ENaC fractions

from the nickel column were then added to the resin and agitated for 30 minutes at room temperature. The supernatant was removed and saved for analysis. The resin was washed 6 times with 0.2 M Tris-HCL, pH 8.0. The protein was then eluted with a 1 M NaCl in 0.2 M Tris-HCl. The tube was agitated for 30 minutes at room temperature. All samples were stored at 4°C.

**Crosslinking**

Purified ENaC was crosslinked with the cleavable crosslinking reagent DTBP (Dimethyl-3-3.-dithiobispropionimidate). Proteins were crosslinked with DTBP using different concentrations and time ranging from 1-5 mM and 5-30 minutes. A 50 mM stock solution of DTBP was made in PBS++ to 12.2 mg DTBP powder. Cells were rinsed 2 times with chilled PBS++, and various amounts of DTBP, were added to cells at room temperature for 30 minutes. The reactions were stopped with the addition of 1.5 M Tris-HCl, pH 8.0.

**Gel Electrophoresis**

**Tris-Glycine SDS-PAGE**

ENaC samples, ~ 44 μg total protein, and 1 X sample buffer (4.0 mL water, 100 mM Tris-HCL, 15 % (v/v) Glycerol, 2% (w/v) SDS, 5 % (v/v) Beta-mercaptoethanol, 0.05% (w/v) bromophenol blue, pH 8.0) were heated for 5 minutes (Thermolyne Type 17600 Dri-bath) at 100°C. Samples were then loaded into individual wells of a 7.5% polyacrylamide gel (BIORAD). Fermentas PageRuler™ prestained

protein ladder was used to estimate molecular weight. Gels were run in 1.5 M Tris-glycine running buffer, pH 8.3, at 135 volts for 60 minutes.

**TAE Agarose Gel**

ENaC samples , ~44 μg total protein, and 1x sample buffer (4.0 mL water, 100 mM Tris-HCL, 15 % (v/v) Glycerol, 2% (w/v) SDS, 5 % (v/v) Beta-mercaptoethanol, 0.05% (w/v) bromophenol blue, pH 8.0.) were heated for 5 minutes at 100°C. Samples were then loaded into individual wells of 5% (w/v) agarose gel. Gels were prepared with a traditional SDS-PAGE apparatus. To prevent the agarose from leaking, 7 % SDS-PAGE was used to seal the apparatus. The agarose was then stored at 4°C overnight in running buffer to prevent the gel from tearing when removing the ladder. Fermentas PageRuler™ prestained protein ladder was loaded into the first lane of every gel. Alternatively, a 2% (w/v) MetaPhor® Agarose gel was also run. Gels were run in 1X TAE buffer (1 M Tris, 0.4 M NaOAc, and 0.04 M EDTA into 1 L water, pH 8 with acetic acid) at 100 volts for 30+ minutes.

**BCA Assay**

BCA assays were used to determine protein concentration. Pierce's BCA Reagent A (7000 μL), (sodium carbonate, sodium bicarbonate, BCA detection reagent and sodium tartrate in 0.1 N sodium hydroxide) was mixed with 140 μL BCA regeant B (copper sulfate). Twenty-five microliters of the following 9 standards were used in each well including 2, 1.5, 1.0, 0.75, 0.5, 0.25, 0.125, 0.025, and 0 mg/mL. BSA amounts 4-8 were taken from previously measured BSA mixtures indicated in parenthesis. To additional

wells, 2.5 µL ENaC and 22.5 µL $dH_20$ were added. To each well 200 µL of BCA mixture was added. The plate was incubated for 15 minutes at 37°C. Absorbance was measured at 562 nm and a standard curve was used to calculate of total protein were concentrations.

**Western Blot**

Proteins were transferred from a SDS-PAGE gel to 0.45 µm nitrocellulose (BIORAD Tras-Blot® Transfer Medium) at 350 mAmps for 1 hour. Transfer buffer contained 1.5 M Tris-Gly and 20% (v/v) methanol. Non-fat milk, 5% w/v, (Sanalac® nonfat dry milk) was used to block the proteins on the nitrocellulose in TBST (20 mM Tris-HCl, pH 7.5, 0.5 M NaCl, 0.05% (v/v) Tween 20) solution for 1 hour. The blot was then incubated at 4-6°C overnight in a 1/1,000 dilution of c-Myc monoclonal antibody in blocking solution. The blot was then washed for 5 minutes with TBST, and incubated in a 1/20,000 dilution of Kirkegaard & Perry Laboratories peroxidase labeled, goat anti-mouse IgG(H+L) in blocking solution for 1 hour while shaking. The blot was washed with TBST three times for 10 minutes. The blot was then washed for 5 minutes with TBS (10 mM Tris-HCl, 150 mM NaCl, pH 7.4). Western Lighting™ chemilumescence reagents, 750 µL oxidizing reagent, and 750 µL enhanced luminal reagent were mixed and incubated on blot for 1 minute. The blot was dabbed dry, taped into a film cassette, and exposed to x-ray film for the desired length of time (1-45 minutes). The film was developed with the AFP Imaging Mini Medical 90 x-ray developer.

## Cell Culture Materials And Methods

### Initiating Cell Culture from Frozen Stock

A frozen vial of COS-1 (P15) cells from the Stockand Laboratory at University of San Antonio Health Science Center was thawed on ice for 15 minutes. The cell vial was incubated at 37°C for 10 minutes and decontaminated with 100% (v/v) ethanol. The cells were pipetted into a culture flask with room temperature complete media [Dulbecco's Modification of Eagles Medium 1 X with (Mediatech Cellgro), L-Glutamine powder (Mediatech Cellgro) Fetal Bovine Serum characterized 40 nm filtered (HyClone®) and Penicillin-Streptomycin 10,000 ug/mL (Mediatech Cellgro™)] and allowed to incubate in a 5 % $CO_2$ incubator at 37°C overnight.

### Passing Cells

Cells were passed when they reached ~100% confluency. Media was removed and cells were washed with Dulbecco's Phosphate Buffered Saline without Mg and Ca. Trypsin (1 X Trypsin EDTA solution 0.05% Trypsin, 0.53 mM without Ca, Mg, $NaHCO_3$ (Mediatech Cellgro™)) was added to the flask and allowed to let sit for 10 minutes. Fresh complete media was added to the flask and pipetted up and down 3 times to remove all cells from the bottom of flask. Cells were placed in a stock flask or Petri dish for experimentation.

# Chapter III

# RESULTS

## Expression of ENaC in COS-1 cells

In order to obtain enough protein for analysis, Green Monkey Kidney Cells (COS-1) were transfected with ENaC expression vectors. The vectors for expression of each ENaC subunit was received from James Stockand at the UT Health Science Center at San Antonio and transformed into competent Top 10$^{TM}$ *E. coli* cells to amplify the amount of plasmid. ENaC constructs of the mammalian expression vector pCMV-Myc were as follows for α-, β-, and γ-ENaC, respectively: pCMV-Myc Alpha-His6, pCMV-Myc Beta, and pCMV-Myc Gamma. Isolated plasmids for each subunit were transfected either individually or in combination into COS-1 cells and protein expression was confirmed via western blot (Figure 5).

ENaC subunits migrated in a 7.5% SDS-PAGE at ~90 kDa. The α-subunit (699 amino acids) and γ-subunit (655 amino acids) migrated together and were difficult to distinguish, whereas the β-subunit (638 amino acids) migrates slightly farther around 80 kDa. Degradation products of these subunits were seen around ~30 kDa.

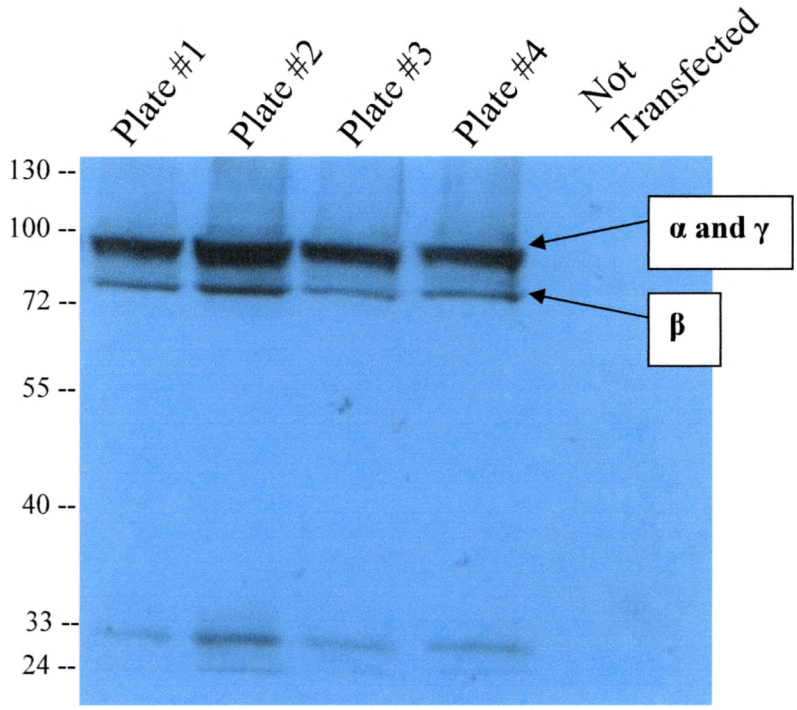


*Figure 5*: **Western Blot of α-, β-, and γ-ENaC Expression** Lanes 1-4: COS-1 cells transfected with pCMV-Myc α-HIS6, pCMV-Myc β, and pCMV-Myc γ-ENaC. Lane 5: whole cell lysate of un-transfected COS-1 cells. Blot was probed with anti-Myc primary and anti-mouse HRP-conjugated secondary antibodies.

## Purification of ENaC

In order to purify ENaC for structural studies, a purification scheme was developed. Multi-subunit complexes of α-, β-, and γ-ENaC were purified from a whole cell lysate using affinity chromatography. Individual subunits and ion were purified from a whole cell lysate using ion-exchange chromatography. Purification of multi-subunit complexes was performed under native conditions (ie., non-denaturing) in order to maintain the subunit-subunit interactions of functional ENaC.

Purification was performed by passing whole cell lysate from transfection of all three subunits through a nickel affinity column to seperate the His6-tagged proteins to

bind to the resin. The flow through that did not have affinity to the nickel resin (Figure 5, lane 1 and 2) ran straight through the column. The bound protein was washed with 50 mM $NaH_2PO_4$, 0.3 M NaCl, pH 8.0 and some non-ENaC proteins were washed out (Figure 6, lane 3). The bound protein was then eluted with 50 mM $NaH_2PO_4$, pH 8.0, with 0.3 M NaCl and 250 mM Imidizole (Figure 6, lane 4). Since non-His6 β- and γ-subunits were associated with the His6-tagged α-subunit, they eluted along with α from the nickel affinity column. A western blot was used to detect ENaC in purification samples including flow through (FT), wash, and elution of the purification steps (Figure 6). The lack of protein in the wash and appearance of ENaC protein in the elution confirms the affinity of the His6-tag for nickel. Gel staining of purified samples showed other proteins have an affinity for the nickel resin (data not shown).

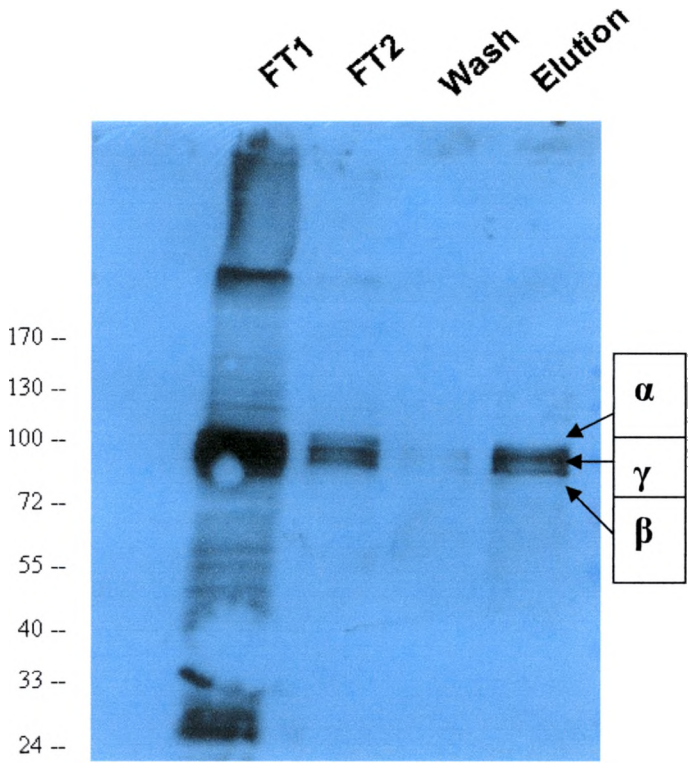


*Figure 6*: **Western Blot of the Purification of ENaC with a Nickel Affinity Chromatography** Lane 1: flow through sample 1 (FT1), Lane 2: flow through sample 2 (FT2), Lane 3: column wash with 50 mM $NaH_2PO_4$, 0.3 M NaCl, pH 8.0, Lane 4: column elution with 50 mM $NaH_2PO_4$, pH 8.0, with 0.3 M NaCl and 250 mM Imidizole. Blot was probed with anti-Myc primary and anti-mouse HRP-conjugated secondary antibodies.

Non-specific binding was in part reduced by adding 5 mM imidazole to the wash buffer. Since complete purification was not achieved, an additional purification step was needed.

All three subunits were transfected individually into COS-1 cells and ran through a CM (cation) and DE52 (anion) exchange column to further purify and determine the overall native charge. The nickel-purified α-His6 subunit was run through both cation and anion resins (anion results not shown). Elution fractions from the nickel affinity column were mixed with 250 uL of either resin, agitated for 30 minutes, and the

supernatant was removed (Figure 7, lane 5). The bound protein was washed with 0.2 M Tris-HCl, pH 8.0 (Figure 7, lane 1 and 2). Protein was eluted with 0.2 M Tris-HCl and 1 M NaCl and was found to bind to the CM cation exchange column (Figure 7, lane 6). Binding of α-His6 ENaC to the cation exchange resin suggests an overall net positive charge due to the abundance of numerous positively charged side chains on the exterior of the α-subunit.

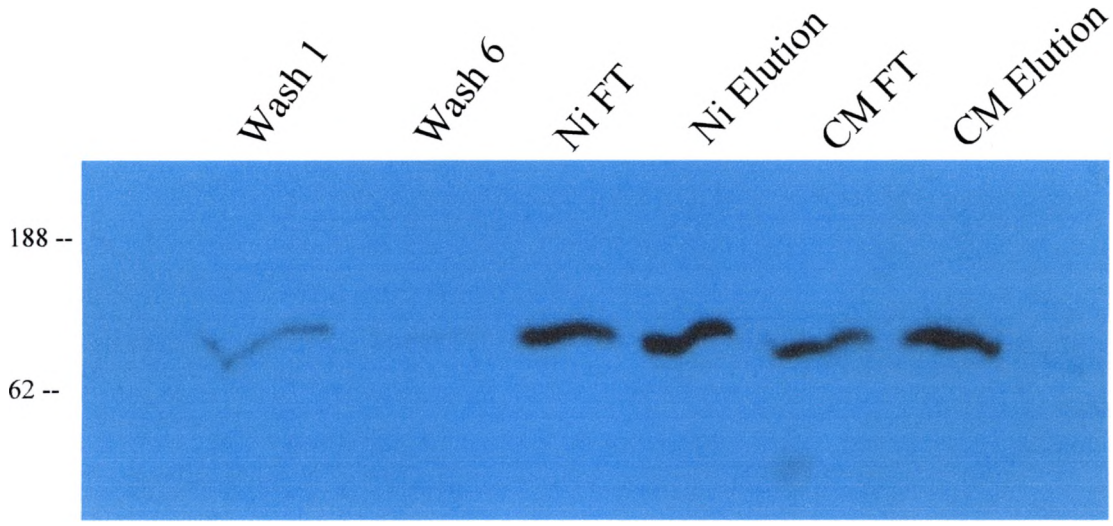


*Figure 7*: **Western Blot of Cation Exchange Chromatography of α-His6 ENaC** Lane 1: Wash #1 with 0.2 M Tris-HCl, pH 8.0, Lane 2: Wash #6 with 0.2 M Tris-HCl, pH 8.0, Lane 3: Nickel affinity column flow-through, Lane 4: Elution with 50 mM $NaH_2PO_4$, pH 8.0, with 0.3 M NaCl and 250 mM Imidizole, Lane 5: CM resin flow through, Lane 6: CM resin elution with 0.2 M Tris-HCl and 1 M NaCl. Blot was probed with anti-Myc primary and anti-mouse HRP-conjugated secondary antibodies.

The β- and γ-subunits were also tested to see which resin they would bind to and determine overall native charge. Both the β- and γ-subunits lack the His6 tag and therefore were not purified using the nickel column. β- and γ-subunits were found to bind to a DE52 anion exchange column and not to the CM cation exchange resin (Figures 8 and 9). Equal amounts of protein were loaded into each gel. Whole cell lysate from the

transfection of the beta subunit was mixed with 250 uL of either resin, agitated for 30 minutes, and the supernatant was removed (Figure 8, lanes 2 and 9). The intensity of the bands is relative to how much protein stuck to the anion exchange resin. The bound protein was washed with 0.2 M Tris-HCl, pH 8.0 (Figure 8, lanes 4-7). Protein was eluted with 0.2 M Tris-HCl and 1 M NaCl and was found to bind to the DE52 anion exchange column and no the cation exchange column (Figure 8, lanes 1 and 8).

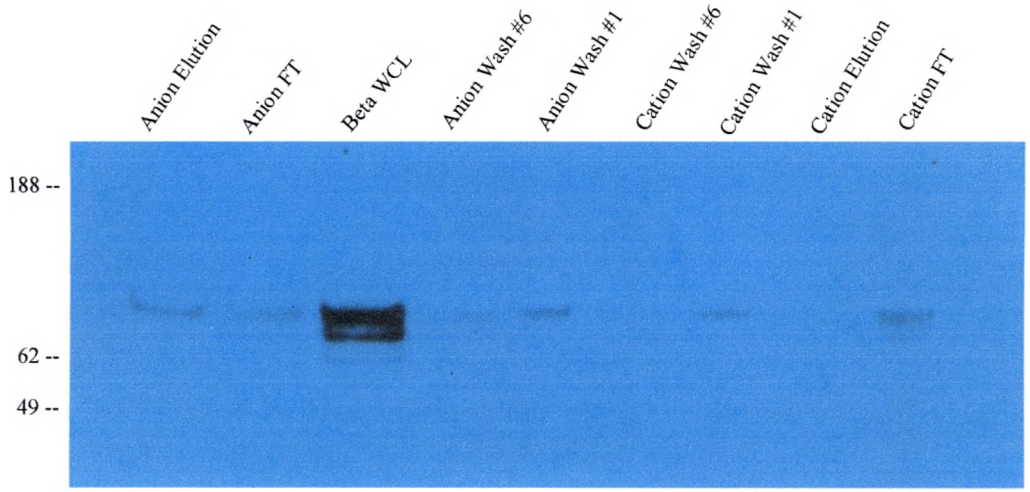


*Figure 8*: **Western Blot of Anion and Cation Exchange Chromatography of β-ENaC** Lane 1: Elution from anion exchange with 0.2 M Tris-HCl, pH 8.0 and 1 M NaCl, Lane 2: Anion exchange flow through, Lane 3: β-ENaC whole cell lysate, Lane 4: Anion exchange wash #6 with 0.2 M Tris-HCl, pH 8.0, Lane 5: Anion exchange wash #1 with 0.2 M Tris-HCl, pH 8.0, Lane 6: Cation exchange wash #6 with 0.2 M Tris-HCl, pH 8.0, Lane 7: Cation exchange wash #1 with 0.2 M Tris-HCL, pH 8.0, Lane 8: Cation exchange elution with 0.2 M Tris-HCl, pH 8.0 and 1 M NaCl, Lane 9: Cation exchange flow through. Blot was probed with anti-Myc primary and anti-mouse HRP-conjugated secondary antibodies.

Whole cell lysate from the transfection of the gamma subunit was mixed with 250 uL of either resin, agitated for 30 minutes, and the supernatant was removed (Figure 9, lanes 2 and 6). The bound protein was washed with 0.2 M Tris-HCl, pH 8.0 (Figure 9, lanes 4 and 5). Protein was eluted with 0.2 M Tris-HCl and 1 M NaCl and was found to bind to

the DE52 anion exchange column and no the cation exchange column (Figure 9, lanes 3 and 7). This suggests that the β- and γ-subunits have a negative surface charge from numerous negatively charged amino acids on their exterior.

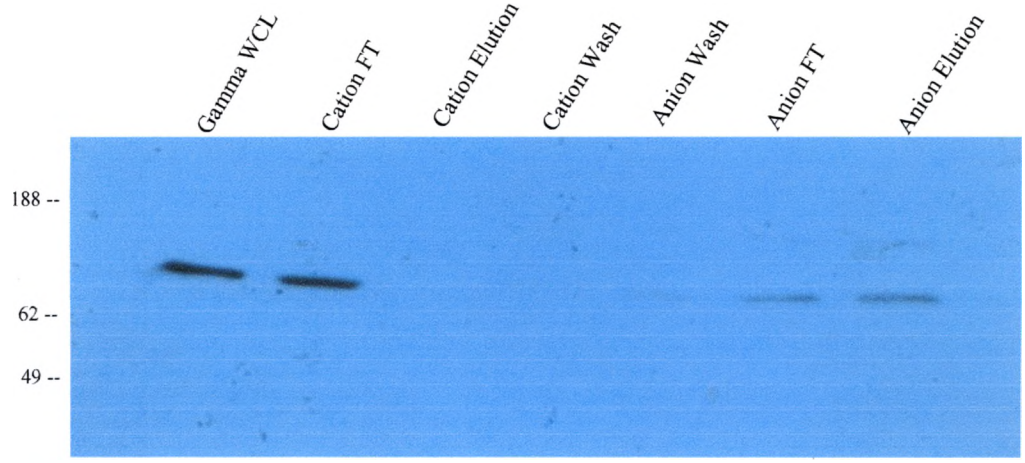


Figure 9: **Western Blot of Anion Exchange and Cation Exchange Chromatography of γ-ENaC** Lane 1: γ -ENaC whole cell lysate, Lane 2: Cation exchange flow through, Lane 3: Cation exchange elution with 0.2 M Tris-HCl, pH 8.0 and 1 M NaCl, Lane 4: Cation exchange wash with 0.2 M Tris-HCl, pH 8.0, Lane 5: Anion exchange wash with 0.2 M Tris-HCl, pH 8.0, Lane 6: Anion exchange flow through, Lane 7: Anion exchange elution with 0.2 M Tris-HCl, pH 8.0 and 1 M NaCl. Blot was probed with anti-Myc primary and anti-mouse HRP-conjugated secondary antibodies.

## Crosslinking

The subunits of ENaC were crosslinked together to determine the molecular weight of a functional channel. The use of a bi-functional reagent as a crosslinker allowed the covalent linking of the subunits together which will not be reduced by components of sample buffer. The crosslinker used was DTBP (Dimethyl-3-3'-dithiobispropionimidate), which contains a cleavable thiol linkage in the spacer arm

(Figure 10). DTBP crosslinks the primary amine on the side chain of the amino acid lysine in close proximity within 11.9 Å. The small spacer arm between the two functional groups of the reagent helped to reduce unwanted crosslinking to non-ENaC proteins.

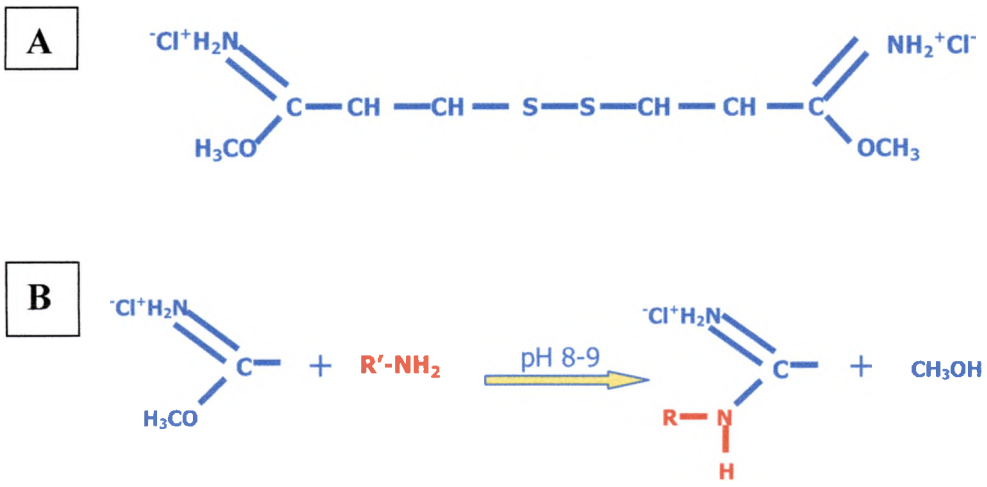


*Figure 10*: **DTBP Structure and Reaction Chemistry** A. Structural formula for dimethyl-3-3'-dithiobispropionimidate (DTBP) showing the cleavable 11.9 Å spacer arm. B. Chemical crosslinking reaction of DTBP with amines on lysine's side chain in close proximity.

ENaC complexes were purified from total cellular proteins and were then crosslinked. Final concentrations of DTBP ranged from 1 mM to 5 mM and were added to the protein in solution and allowed to incubate at room temperature for 30 minutes. The reaction was stopped with the addition of 1.5 M Tris-HCl, pH 8.0. The disappearance of ENaC subunit intensity as the concentration of crosslinker increased from 1 mM to 5 mM shows that the subunits were crosslinked and formed large complexes. These complexes were unable to enter the 7.5 % SDS-PAGE gel matrix (Figure 11, lanes 2-6). This indicated that the combined molecular weight if the linked complex might be larger than the proposed 4-subunit model of 360 kDa.

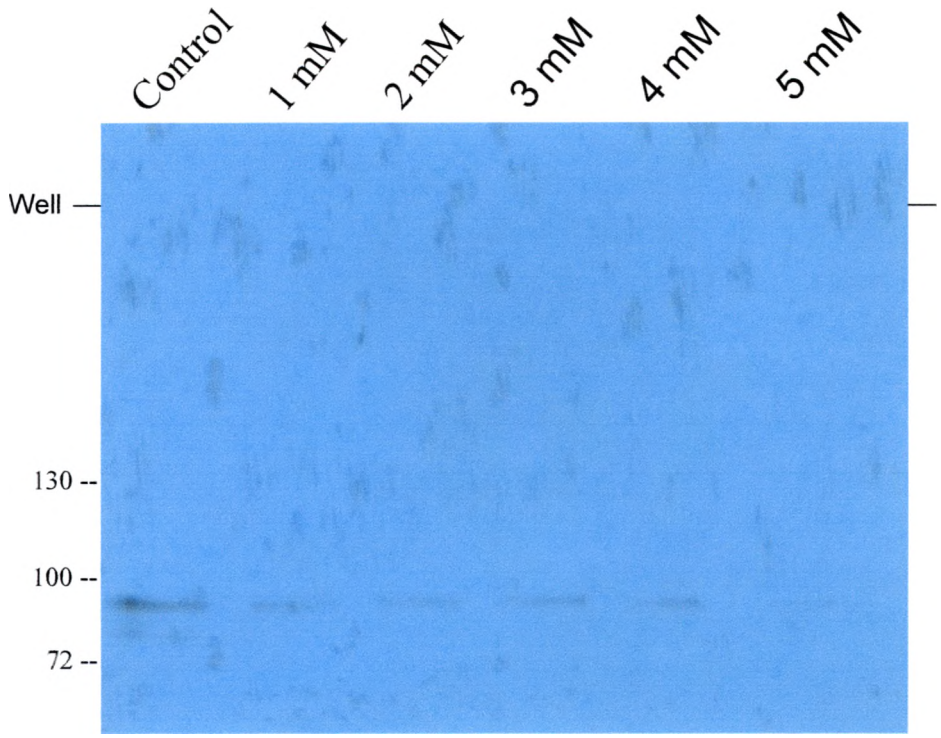


*Figure 11*: **Western Blot of ENaC Crosslinked with Varying Concentrations of DTBP** Lane 1: All three subunits not crosslinked, Lane 2: All three subunits crosslinked with 1 mM DTBP, Lane 3: All three subunits crosslinked with 2 mM DTBP, Lane 4: All three subunits crosslinked with 3 mM DTBP, Lane 5: All three subunits crosslinked with 4 mM DTBP, Lane 6: All three subunits crosslinked with 5 mM DTBP. Blot was probed with anti-Myc primary and anti-mouse HRP-conjugated secondary antibodies.

By using DTBP, we were able to then cleave the thiol linkage to confirm the reaction, and determine if any smaller complexes would then migrate into the gel. ENaC complexes were crosslinked with 3 mM DTBP for 30 minutes, then stopped with the addition of 1.5 M Tris-HCl, pH 8.0 (Figure 12, lane 1). Crosslinked linkages were broken with 70 mM DTT (Figure 12, lane 2).

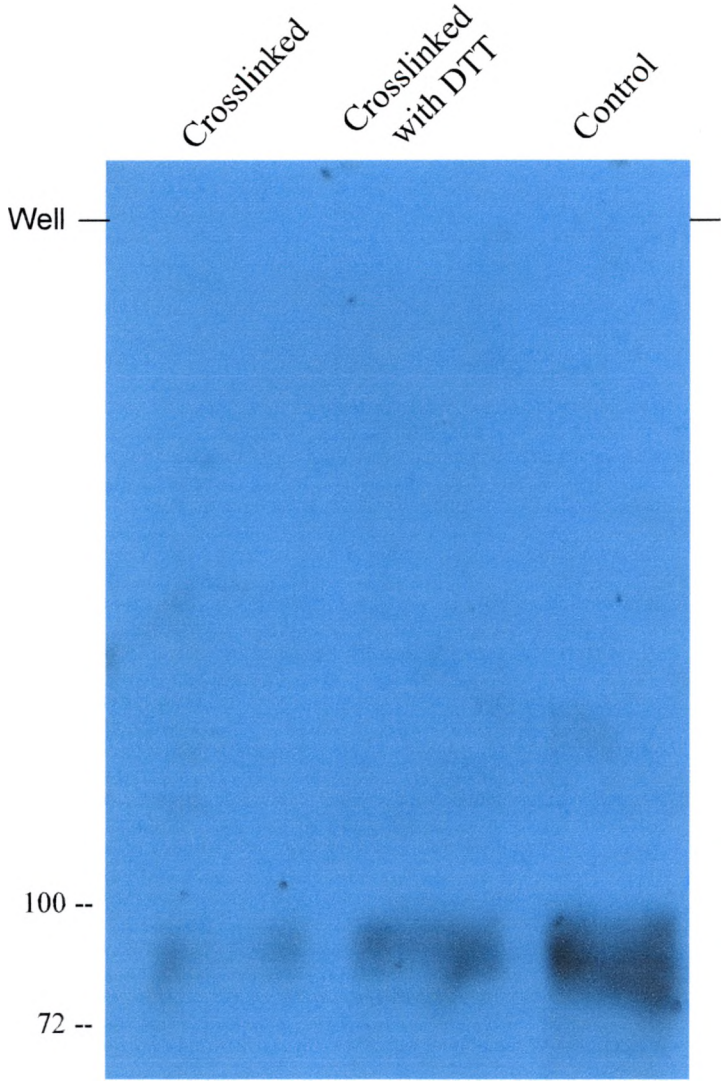


*Figure* 12: **Western Blot of Crosslinked ENaC Complex** Lane 1: All three subunits crosslinked with 10-molar excess DTBP, Lane 2: Crosslinked linkages broken with 70 mM DTT, Lane 3: All three subunits not crosslinked. Blot was probed with anti-Myc primary and anti-mouse HRP-conjugated secondary antibodies.

The reappearance of monomeric subunits upon the addition of DTT shows that the spacer arm of DTBP holding the subunits together was cleaved (Figure 12, lane 2). Upon cleavage of crosslinked subunits, we expected ENaC complexes to migrate in the 360-400 kDa range. No ENaC was found in this range.

ENaC complexes were then crosslinked with a final concentration of 5 mM DTBP for 30 minutes and stopped with the addition of 1.5 M Tris-HCl, pH 8.0 (Figure 13, lane 5). Crosslinked complexes were then treated with various amounts of DTT to possibly visualize any complexes formed by cleaving the crosslinking. The thiol linkage in DTBP's spacer was arm was cleaved with concentrations of DTT ranging from 1.3 mM to 5 mM (Figure 13, lanes 1-4).

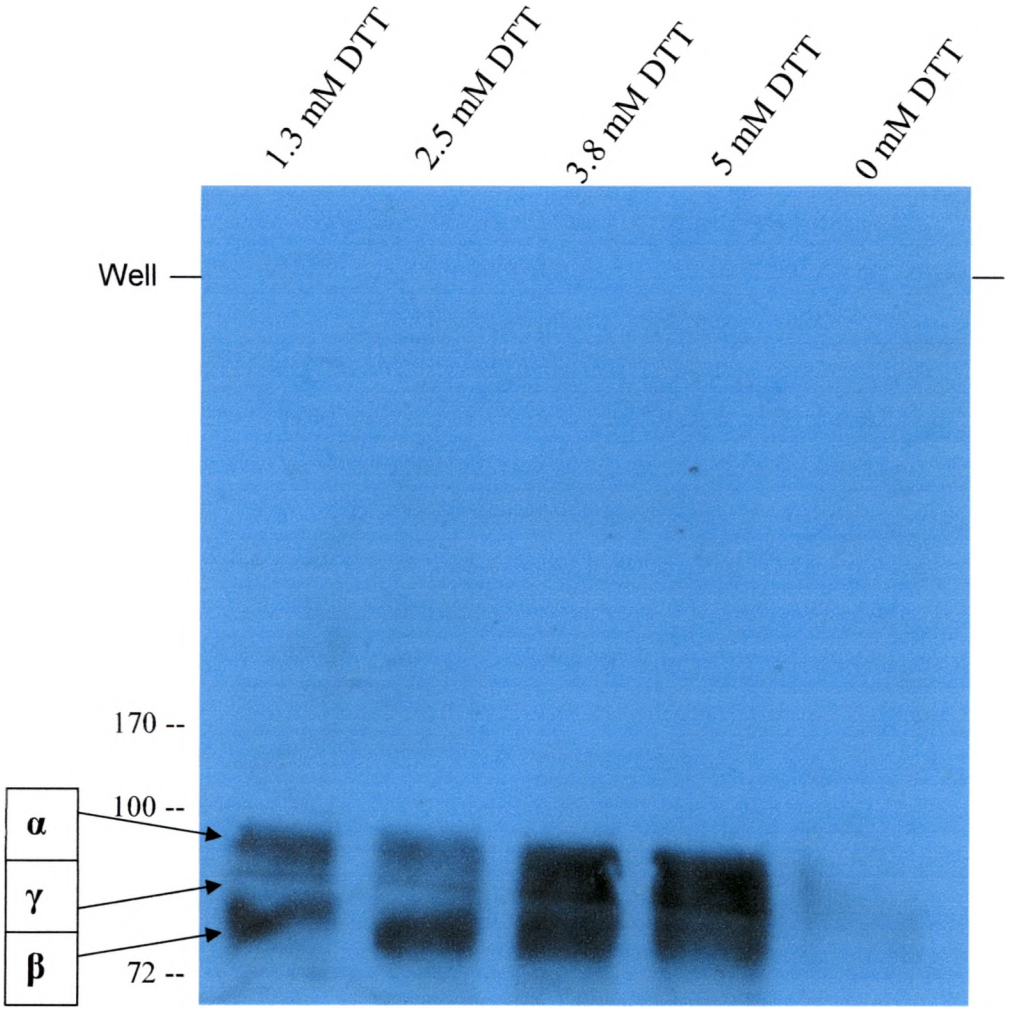


*Figure 13*: **Western Blot of the Cleavage of Chemically Crosslinked Subunits Treated with DTT** Crosslinked samples were cleaved for 30 minutes in the presence of 0 mM (lane 1), 1.3 mM (lane 2), 2.5 mM (lane 3), 3.8 mM (lane 4), and 5 mM (lane 5). Blot was probed with anti-Myc primary and anti-mouse HRP-conjugated secondary antibodies.

In an effort to resolve the ENaC crosslinked complexes, the crosslinked protein was run in a 5% (w/v) agarose gel, which can resolve ~500 kDa molecular weight molecules. Preliminary experiments by an undergraduate in our lab ran standards in the same agarose setup that were used for these experiments. It was found that a standard of roughly 500 kDa would migrate down a 5% (w/v) agarose gel. The gels were poured in a traditional SDS-PAGE apparatus and were also transferred to nitrocellulose and developed in the same manner as the SDS-PAGE. ENaC complexes were crosslinked with a final concentration of 5 mM DTBP and stopped with the addition of 1.5 M Tris-HCl, pH 8.0 (Figure 14, lane 2). The 5% (w/v) agarose crosslinked ENaC complexes were seen just below the well of the gel (Figure 14). The control (Figure 14, lane 1) is the uncrosslinked individual subunits, while lane 2 shows the short migration of the crosslinked complex into the agaroses' matrix.

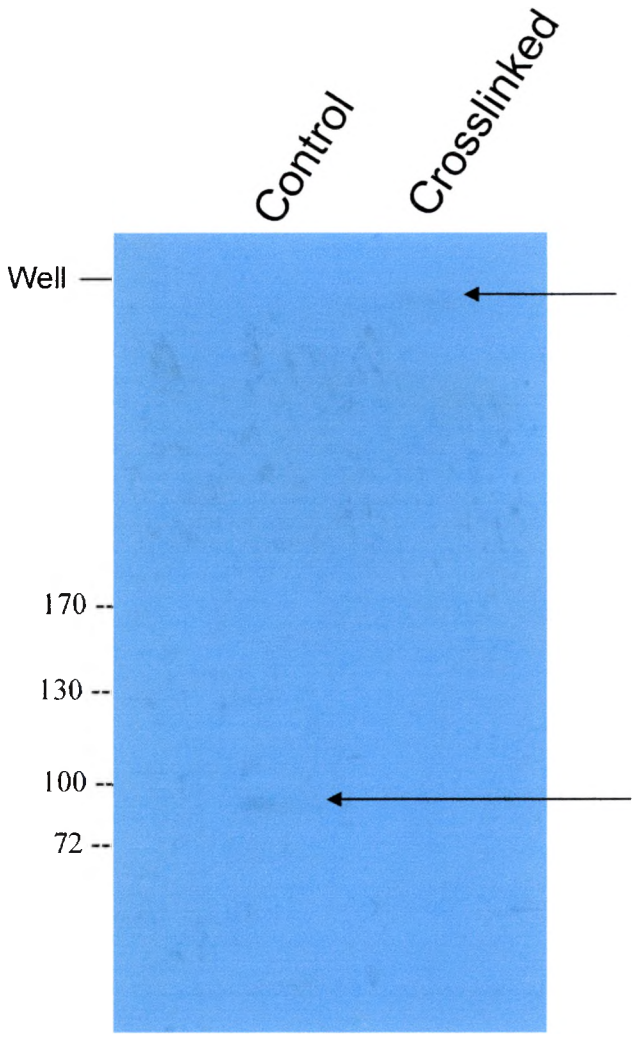


*Figure 14:* **Western Blot of Crosslinked ENaC in a 5% (w/v) Agarose Gel** Lane 1: ENaC not cross-linked, Lane 2: Cross-linked ENaC with DTBP. Blot was probed with anti-Myc primary and anti-mouse HRP-conjugated secondary antibodies.

MetaPhor® Agarose, a high resolution agarose that has been used to separate ~500 kDa proteins, was also employed to resolve the crosslinked complexes (Figure 15). ENaC complexes were crosslinked with a final concentrations of DTBP ranging from 1 mM to 5 mM for 30 minutes, and stopped with the addition of 1.5 M Tris-HCl, pH 8.0 (Figure 15, lanes 1-5). Although MetaPhor® has twice the resolution capabilities for large molecules when compared to other agarose products, the ENaC complexes migrated just

below the wells. Even with a very low percentage gel of 2% (w/v), the crosslinked complexes do not migrate far into the gel matrix.

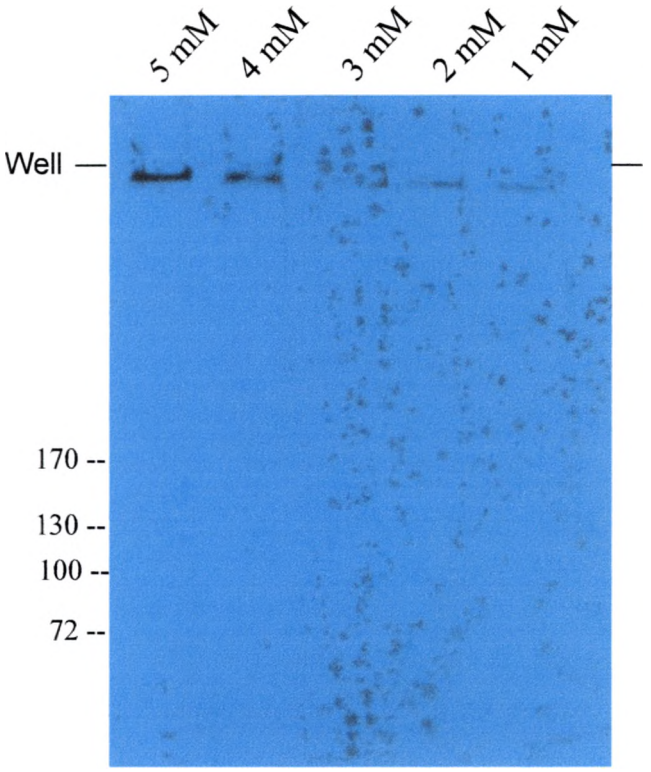


*Figure 15:* **Western Blot of Crosslinked Complexes in a 2% MetaPhor® Agarose Gel** ENaC crosslinked with DTBP for 30 minutes with a concentration of 5 mM (lane 1), 4 mM (lane 2), 3 mM (lane 3), 2 mM (lane 4), and 1 mM (lane 5). Blot was probed with anti-Myc primary and anti-mouse HRP-conjugated secondary antibodies.

The expected migration of a band for the 4-subunit model in MetaPhor® Agarose was ~360 kDa. We would have seen this size migrate into the 2% (w/v) MetaPhor® Agarose gel (Figure 15).

**Sequence Alignment and Secondary Structure**

In order to show the similarity between the primary amino acid sequences of the subunits, a sequence alignment comparison was performed. The gene sequences of all three subunits from mouse were compared to each other to show similarities. Sequence alignment data was retrieved from ClustalW (http://www.ebi.ac.uk/clustalw/), a multiple sequence alignment program that calculates the best match for the selected sequences showing their identities, similarities, and differences. All three subunits were compared for homologous and conserved residues. An alignment display denoting the degree of conservation in each column was observed. There are few gaps between the comparisons of the three subunits against each other, showing a high degree of similarity in amino acid sequence (Figure 16). Homology was found to be 33 % and similarity was 55 %.

```
Beta            ------------------------------------------------------MPVK  4
Gamma           ------------------------------------------------------MAPGE  5
Alpha           MLDHTRAPELNLDLDLDVSNSPKGSMKGNNFKEQDLCPPLPMQGLGKGDKREEQALGPEP  60
                                                                        *

Beta            KYLLKCLHRLQKG--PGYTYKELLVWYCNNTNTHGPKRIICE--GPKKKAMWFLLTLLFA  60
Gamma           KIKAKIKKNLPVRGPQAPTIKDLMHWYCLNTNTHGCRRIVVSR-GRLRRLLWIAFTLTAV  64
Alpha           SEPRQPTEEEEALIEFHRSYRELFQFFCNNTTIHGAIRLVCSKHNRMKTAFWAVLWLCTF  120
                .   :  ..         : ::*: ::* **. **  *:: .  .  :  :*  . *

Beta            CLVCWQWGVFIQTYLSWEVSVSLSMGFKTMNFPAVTVCNSSPFQYSKVKHLLKDLDELME  120
Gamma           ALIIWQCALLVFSFY--TVSVSIKVHFQKLDFPAVTICNINPYKYSAVSDLLTDLDSETK  122
Alpha           GMMYWQFALLFEEYFSYPVSLNINLNSDKLVFPAVTVCTLNPYRYTEIKEDLEELDRITE  180
                 :: ** .::.  : :  **:.:.:  ..: *****:*. .*::*: :.. * :**   :

Beta            AVLEKILAPEASHSNTTRTLN-----FTIWNHTP-------LVLIDERNPDHPVVLNLFG  168
Gamma           QALLSLYGVKDVLDSTPRKRREAGSMRSTWEGTPPRFLNLIPLLVFNENEKGKARDFFTG  182
Alpha           QTLFDLYKYNSSYTRQAGGRR-----RSTRDLRG-------ALPHPLQRLRTPPPPNPAR  228
                 .* .:   :      .   .      :  :           :    ..

Beta            DSHNSSNPAPGSTCNAQGCK-----VAMRLCSANGTVCTLRNFTSATQAVTEWYILQATN  223
Gamma           RKRKISGKIIHKASNVMHVHESKKLVGFQLCSNDTSDCATYTFSSGINAIQEWYKLHYMN  242
Alpha           SARSASSSVRDNNPQVDRKD---WKIGFQLCNQNKSDCFYQTYSSGVDAVREWYRFHYIN  285
                  :. *.    .  :.   .     :.::**. : : *   .::*. :*: *** ::  *

Beta            IFSQVLPQDLVGMGYAPDRIILACLFGTEPCSHRNFTPIFYPDYGNCYIFNWGMTEETLP  283
Gamma           IMAQVPLEKKINMSYSAEELLVTCFFDGMSCDARNFTLFHHPMYGNCYTFNNRENATILS  302
Alpha           ILSRLPDTSPALEEEALGSFIFTCRFNQAPCNQANYSQFHHPMYGNCYTFNNKNNSNLWM  345
                *::::   .      :   ::.:* *.  .*.  *:: :.:* ***** **   .

Beta            SANPGTEFGLKLILDIGQEDYVPFLASTAGARLMLHEQRTYPFIREEGIYAMAGTETSIG  343
Gamma           TSMGGSEYGLQVILYINEDEYNPFLVSSTGAKVLVHQQNEYPFIEDVGTEIETAMSTSIG  362
Alpha           SSMPGVNNGLSLTLRTEQNDFIPLLSTVTGARVMVHGQDEPAFMDDGGFNVRPGVETSIS  405
                ::  * : **.: *   :::: *:* : :**::::* *   .*: : *    .. .***.

Beta            VLVDKLQRKGEPYSPCTMNGSDVAIKNLYSVYNTTYSIQACLHSCFQDHMIRNCSCGHYL  403
Gamma           MHLTESFKLSEPYSQCTEDGSDVPVT---NIYNAAYSLQICLYSCFQTKMVEKCGCAQYS  419
Alpha           MRKEALDSLGGNYGDCTENGSDVPVK---NLYPSKYTQQVCIHSCFQENMIKKCGCAYIF  462
                :        .  *. ** :****.:.   .:* : *: * *::**** :*:.:*.*.

Beta            YPLPEGEKYCNNRDFPDWAYCYLNLQMSVTQRET-CLSMCKESCNDTQYKMTISMADWPS  462
Gamma           QPLPPAANYCNYQQHPNWMYCYYQLYQAFVREELGCQSVCKQSCSFKEWTLTTSLAQWPS  479
Alpha           YPKPKGVEFCDYLKQSSWGYCYYKLQAAFSLDSLGCFSKCRKPCSVTNYKLSAGYSRWPS  522
                 * * . ::*:  . ..* *** :*  :.   . .* * *::.*. .::.:: . : ***

Beta            EASEDWILHVLSQERDQSSNITLSRKGIVKLNIYFQEFNYRTIEESPANNIVWLLSNLGG  522
Gamma           EASEKWLLNVLTWDQSQQINKKLNKTDLAKLLIFYKDLNQRSIMESPANSIEMLLSNFGG  539
Alpha           VKSQDWIFEMLSLQNNYTINNKRN--GVAKLNIFFKELNYKTNSESPSVTMVSLLSNLGS  580
                  *:.*::.:*: :..   * . .  .:.** *:::::* ::  ***: .:  ****:*.

Beta            QFGFWMGGSVLCLIEFGEII--IDFIWITIIKLVASCKGLRRRRPQAPYTGPPPTVAELV  580
Gamma           QLGLWMSCSVVCVIEIIEVFF-IDFFSIIARRQWQKAKDWWARRRTPPSTETPSSQQGQD  598
Alpha           QWSLWFGSSVLSVVEMAELIFDLLVITLIMLLHRFRSRYWSPGRGARGAREVASTPASSF  640
                * .:*:. **:.::*: *:: .: .: :        .:     *        ..:

Beta            EAHTNFGFQPDTTSCRPHGEVYPDQQTLPIPGTPPPNYDSLRLQ-PLDTMESDSEVEAI-  638
Gamma           NPALDTDDDLPTFTSAMR---LPPAPEAPVPGTPPPRYNTLRLDSAFSSQLTDTQLTNEF  655
Alpha           PSRFCPHPTSPPPSLPQQGTTPPLALTAPPPAYATLGPSASPLDSAVPGSSACAPAMAL-  699
                 .         . :   :.   *     * *. ..   .:  *::..    : :
```

*Figure 16:* **Homologous and Conserved Residues Between Alpha, Beta, and Gamma** (*) Denotes residues or nucleotides in that column are identical in all sequences in the alignment. (:) Denotes that conserved substitutions have been observed. (.) Denotes that semi-conserved substitutions are observed.

To determine any similarities or differences in secondary structure of the three subunits, their predicted secondary structure was analyzed. Amino acid sequence analysis using GOR IV Secondary Structure Prediction Method (http://.ca.expasy.org/tools/#secondary) was performed in order to compare and contrast secondary structures of each subunit. Through close comparison, all three subunits are very similar in their predicted percentages of secondary structure (Table 1). They came to be within: 7 % random coil of each other, 8 % beta sheet of each other, and 13 % alpha helix of each other.

*Table 1.* **Predicted Secondary Structures for Alpha, Beta, and Gamma Subunits**

| Subunit: | Sequence Length | Alpha Helix | Beta Sheet | Random Coil |
|---|---|---|---|---|
| Alpha | 699 a.a. | 21.32% | 20.17% | 58.51% |
| Beta | 638 a.a. | 14.89% | 28.53% | 56.58% |
| Gamma | 655 a.a. | 27.02% | 21.37% | 51.60% |

For the alpha subunit to have a different overall net charge as we suggest from the cation and anion exchange chromatography, differences may exists in the subunits tertiary fold. These results may suggest that alpha folds differently than beta or gamma, yielding a different exterior charge and channel functionality characteristics.

## Chapter IV

## DISCUSSION

Structure-function relationships are important in understanding their central role in many biological processes. Examining ENaC's structure through the use of traditional biochemistry techniques including protein purification and chemical crosslinking have helped us to understand some of ENaC's structure-function relationships.

The epithelial sodium channel is a pore forming protein channel responsible for the maintenance of blood homeostasis. The main issue in structural studies of ENaC is obtaining sufficient amounts of the proteins. This is because first of all, ENaC is only made in the cell when needed and second, we are dealing with a membrane bound protein. A purification scheme was developed in order to purify ENaC for future studies. All subunits were co-purified with the nickel affinity column. The nickel-purified protein complex was further purified with a cation exchange column to eliminate non-ENaC proteins. Since the alpha subunit binds to CM cation exchange resin and not to an anion exchange resin, this suggests the presence of certain amino acids on the exterior of the subunit, and an overall net positive charge. In this case, lysine and arginine, positively charged amino acids, are likely to be abundant on the outer region of the alpha subunit. Histidine's pKa of 6.04 is below the pH of the reaction conditions (8.0), so histidine will have a neutral charge, not contributing to the overall net positive charge. Our findings in this aspect are also consistent with Sheng *et al.* who found that by mutating residues to negatively charged residues on the alpha subunit significantly reduced $Na^+$ currents (20).

This is in agreement with our findings in that the alpha subunit has a positively charged exterior. ENaC subunits share a 34-37 % identity, and a 51 % homology in protein sequence (4). This shows that the subunits are 34-37 % similar in their amino acid makeup, thus may fold differently to have different charged exterior residues. In contrast to the alpha subunit, the beta and gamma subunits were found to bind to an anion exchange column. This indicates that they have negatively charged amino acids, e.g. glutamatic acid and aspartic acid, on their exterior. Also, since alpha is the only subunit found to have a mainly positively charged exterior, this may suggest that it is found between each beta and gamma subunit. If this is true, the channel would have an alternating stiochometry with an alpha subunit in between every beta and gamma subunit.

Ishikawa *et al.* found that through using patch clamp analysis, channels consisting of $\alpha\beta$ or $\alpha\gamma$ subunits alone created a whole-cell $Na^+$ current close to untransfected cells (9). In addition, Ismailov *et al.* found that through planar lipid bilayer studies neither $\beta$ nor $\gamma$ can form functional channels alone (10). This previous research illustrates how important alpha is in proper channel function. Since the subunits are very similar in their amino acid makeup, our exterior charge findings, and a prediction of secondary structure, helps suggest alpha is folded differently than beta and gamma. This would expose different residues on the exterior of alpha giving alpha the different exterior charge. Previous studies have mutated histidine residues on the alpha subunits' extracellular loop which were found to bind to amiloride. When the positive charge (histidine) was mutated to aspartic acid (negatively charged amino acid), a 39 fold increase in amiloride sensitivity was recorded. When the histidine was mutated to arginine, conserving the cationic charge, there was only a 6-fold decrease in sensitivity for amiloride. Although in

our experiments histidine had a neutral charge because of our reaction pH, conditions on the extracellular loop of alpha could promote histidine to become positively charged if below a pH of 6.04. This helps support our results in that alpha, the predominant subunit, has exterior positively charged amino acids, which when one is mutated to a negatively charged amino acid, looses the important role of stabilizing the binding of amiloride to the sodium channel (10).

Weisz *et al.* have shown in their work that the three subunits of ENaC are synthesized in a different fashion from one another, having 1-2 subunits expressed constitutively, while the other(s) may be induced by different stimuli (23). Other previous reports have shown that beta and gamma subunits by themselves are not expressed at the plasma membrane (2). Our work is consistent with their finding in regards to the exterior charge difference of alpha to beta/gamma. The difference in expression would fit that beta and gamma are constitutively expressed at the same time, while alpha is only expressed if the correct stimuli is created. Since alpha would be made using a different mechanism, differences in the folding of its secondary structure are possible.

Beta and gamma ENaC can be substitute for each other to form functional channels (5). Our findings may be consistent with the lab of McNicholas *et al.* who found that αβ channels expressed a slightly larger $Na^+$ and $Li^+$ current than did αγ channel (17). This shows that as long as the alpha subunit is present, the addition of either beta or gamma produces an equivalent channel. We are suggesting that beta and gamma, because of charge, can be substituted for each other within the channels' stoichiometry.

Due to the exterior charge of the individual subunits, and our suggestions on the channel stoichometry, beta and gamma could be readily interchangeable around alpha. Beta exists as the smaller subunit (Figure 5), yet has a close similarity with the gamma subunits' amino acid makeup and folding patterns.

Crosslinking the ENaC subunits demonstrated that the complexes formed were larger than the 4-subunit model at ~360 kDa. Previous work in our lab involved running standards in a 2% (w/v) MetaPhor® Agarose with the findings that proteins up to ~500 kDa migrate into the matrix. Unfortunately, the cross-linked samples were not suitable for molecular weight determination via SDS-PAGE gels. Since the crosslinked complex can exist in many different arrangements, according to the reagents spacer arm, concentration of reagent, and time allowed, predictions of exact crosslinks is not feasible.

Kosari *et al.* and Firsov *et al.* have proposed a 4 subunit model for ENaC with a subunit ratio of 2α: 1β: 1γ (5, 12). Our crosslinking findings are not consistent with suggesting a 4 subunit model because we did not see migration of a ~360 kDa band in the SDS-PAGE or agarose gels. Snyder *et al.* and Eskandari *et al.* proposed a 9 subunit model for ENaC consisting of a subunit ratio of 3α: 3β: 3γ (3, 22). Our findings are more consistent with their work in that our work suggests that ENaC is composed of more than 4 subunits. Concentration dependent cleavage of chemically crosslinked ENaC does not result in complexes in the 200-400 kDa range as seen in Figure 14. The inability of the crosslinked complexes to enter even the matrix of agarose, which will allow entrance of ~500 kDa proteins, provides evidence for our suggestion. This aids our suggestion that ENaC exists in a stoichometry of greater than 4 subunits, most likely 9-subunit model.

## Chapter V

## CONCLUSIONS

The epithelial sodium channel and individual subunits have been partially purified in this study. Although it takes several steps for purification, they are synergistic in eliminating non-ENaC proteins. Due to the higher purity of ENaC found after purifying with nickel, cation, and anion exchange columns, future structural studies will benefit from this purity.

Examination of the crosslinked complexes in SDS-PAGE and agarose gels before and after cleaving the spacer arm of DTBP has suggested several ideas characteristic of structure for ENaC. The crosslinked samples size suggests that ENaC exists in a stiochometry larger than 4 subunits. The large crosslinked complex exists in a size larger that 500 kDa which will not migrate into the matrix of the SDS-PAGE or agarose gels. The 4-subunit model would have a combined weight of 360 kDa. This would have entered the Agarose setup, yet the complex did not which suggests that ENaC exists in a stiochometry larger than only 4 subunits. A different type of gel apparatus will have to be employed in order for these large crosslinked complexes to be resolved, possibly a large-scale SDS-PAGE setup will resolve these large complexes. The subunits are also in very close proximity to each other, within at least 11.9 Å of each other.

The finding of the alpha subunit to bind to a cation exchange column and beta/gamma to bind to an anion exchange column has suggested a majority of the exterior amino acid identities. This could possibly mean a high concentration of lysine or arginine, on the outer surface of the three-dimensional shape of the alpha subunit, and a

high concentration of glutamate acid and/or aspartic acid for beta and gamma. These findings also lead us to believe that ENaC is composed of an alternating stoichometry of alpha in between every beta and gamma subunit. This also leads to the generalization that gamma and beta are not found next to each other, and can possibly substitute for each other in the channels' stoichiometry. Due to the subunits' amino acid similarity with each other, alpha may fold differently from beta and gamma giving it different characteristics.

The results of this study have provided a purification procedure for future structural studies of this channel. Also, these findings will help aid future studies using our suggestions of the channels stiochometry and the exterior subunit amino acid identities. In future studies, isolated proteins from this work will be analyzed via mass spectrophotometer analysis in order to identify additional motifs in ENaC that can be manipulated and functionally characterized. These future findings will give insight to ENaC's role in several cardiovascular diseases.

## REFERENCES

Canessa, C.M., and Gupta, S.S., 2000. Heterologous expression of a mammalian epithelial sodium channel in yeast. *FEBS Letters.* 481:77-80.

Canessa, C.M., Horisberger, J.D., and Rossier, B.C., 1993. Epithelial sodium channel related proteins involved in neurodegeneration. *Nature (Lond)* 361:467-470.

Eskandari, S., Snyder, P.M., Kreman, M., Zampighi, G.A., Welsh, M.J., and Wright, E.M., 1999. Number of subunits comprising the epithelial sodium channel. *The J of Biol.Chem.* 274:27281-27286.

Farman, N., Talbot, C.R., Bouchner, R.C., Canessa, C.M., Rossier, B.C., and Bonvalet, J.P., 1997. Non-coordinated expression of [alpha], [beta], and [gamma] subunit mRNAs of the epithelial sodium channel along the rat respiratory tract. *Am J Physiol.* 272:131-141.

Firsov, D., Gautschi, I., Merillat, A., Rossier, B.C., and Schild, L., 1998. The heterotetrameric architecture of the epithial sodium channel (ENaC). *The EMBO J.* 17:344-352.

Fyfe, G., and Canessa, C.M., 1998. Subunit composition determines the single channel kinetics of the epithelail sodium channel. *J Gen. Physiol.* 112:423-432.

Hanwell, D., Ishikawa, T., Saleki, R., and Rotin, D., 2002. Trafficking and cell surface stability of the epithelial Na+ channel expressed in epithelial madin-darby canine kidney cells. *The J. of Biol. Chem.* 227:9772-9779.

Hendron, E., Patel, P., Hausenfluke, M., Gamper, N., Shapiro, M.S., Booth, R.E., and Stockand, J.D., 2002. Identification of cytoplasmic domains within the epithelial $Na^+$ channel reactive at the plasma membrane. *The J. of Biol. Chem.* 227:34480-34488.

Ishikawa, T., Marunaka, Y., and Rotin, D., 1998. Electrophysiological Characterization of the Rat Epithelial Na+ Channel (rENaC) Expressed in MDCK Cells. *J Gen. Physiol.* 111:825-846

Ismailov, I., Awayda, M.S., Berdiev, B.K., Bubien, J.K., Lucas, J.E., Fuller, C.M., and Benos, D.J., 1996. *J* Triple-barrel organization of ENaC, a cloned Epithelial $Na^+$ Channel. *Biol. Chem.* 271:807-816

Kanelis V., Rotin, D., and Forman-Kay, J. D., 2001. Solution structure of a Nedd4 WW domain-ENaC peptide complex. *Nat. Struct. Biol.* 8:407-412.

Kosari, F., Sheng, S., Li, J., Mak, D.O., Foskett, J.K., and Kleyman, T.R., 1998. Subunit stoichiometry of the epithelial sodium channel. *The J. of Biol. Chem.* 273:13469-13474.

Li, J., Sheng, S., Perry, C.J., and Kleyman, T.R., 2003. Asymmetric orgination of the pore region of the epithelial sodium channel. *The J. of Biol. Chem.* 278:13867-13874.

Lifton, R.P., 1995. Genetic determinants of human hypertension. *Proc. Natl. Acad. Sc USA.* 92:8545-8551.

Lifton, R.P., 1996. Molecular genetics of human blood pressure variation. *Science.* 272:676-680.

Lifton, R.P., Gharavi, A.G., and Geller, D.S., 2001. Molecular mechanisms of human hypertension. *Cell.* 104:545-556.

McNicholas, C.M., and Canessa, C.M., 1997. Diversity of channels generated by different combinations of epithelail sodium channel subunits. *J. Gen Physiol.* 109:681-692.

Rosa, D.A., Canessa, C.M., Fyfe, G.K., and Zhang, P., 2000. Structure and regulation of amiloride-sensitive sodium channels. *Annu Rev. Physiol.* 62:573-94.

Sheng, S., Li, J., McNulty, K.A., Kieber-Emmons, T., and Kleyman, T.R., 2001. Epithelial sodium channel pore region. *The J. of Biol Chem.* 276:1326-1334.

Sheng, S., McNulty, K.A., Harvey, J.M., and Kleyman, T.R., 2001. Second transmembrane domains of ENaC subunits contribute to ion permeation and selectivity. *The J. of Biol. Chem.* 276:44091-44098.

Shimkets, R.A., Lifton, R.P., and Canessa, C. M., 1997. The activity of the epithelial sodium channel is regulated by clathrin-mediated endocytosis. *The J. of Biol. Chem.* 272:25537-25541.

Snyder, P.M., Cheng, C., Prince, L.S., Rogers, J.C., and Walsh, M.J.,1997. Electrophysiological and biochemical evidence that DEG/ENaC cation channels are composed of nine subunits. *The J. of Biol. Chem.* 273:681-684.

Weisz, O., and Johnson J.P., 2003. Noncoordinate regulation of ENaC: paradigm lost? *Am J. Physiol Renal Physiol.* 285:833-842.

# VITA

Sean Larson Schmidt was born in Fredericksburg, Texas, on July 16, 1979, the son of Larry Lee Schmidt and Cheryl La'Mae Schmidt. After graduating from Boerne High School in 1998, he attended Texas State University-San Marcos from August 1998 thru May 2003 and graduated with a Bachelor of Science degree with a major in biology and a minor in chemistry. Starting in August 2003, he began graduate school in the Department of Chemistry and Biochemistry at Texas State University-San Marcos.

Permanent Address: 446A Hwy 46E

Boerne, TX 78006

This thesis was typed by Sean Larson Schmidt.